Journal of Materials Science: Materials in Electronics (2018) 29:13687–13691
https://doi.org/10.1007/s10854-018-9497-y

Bipolar resistance switching properties of pulse laser deposited a-ZrO_2/a-IGZO transparent heterojunction

Bhaumik V. Mistry[1] · **U. S. Joshi**[1]

Received: 13 March 2018 / Accepted: 16 June 2018 / Published online: 27 June 2018

Abstract
Transparent resistive switching characteristics of amorphous ZrO_2 (a-ZrO_2) based memory film with amorphous In and Ga co-doped ZnO (a-IGZO) conducting electrode were investigated. a-ZrO_2/a-IGZO heterojunction was fabricating using pulse laser deposition techniques on quartz substrate. Structural, surface, electrical, and optical properties of a-ZrO_2/a-IGZO heterojunction were investigated at room temperature. Smooth surface morphology and amorphous nature of the structure has been confirmed from the atomic force microscopy (AFM) and grazing incident X-ray diffraction (GIXRD) analysis. a-ZrO_2/a-IGZO heterojunction has optical transmission exceeding 80% in visible light of electromagnetic spectrum. *I–V* characteristics show a forming free, bipolar resistance switching type behavior. Migration of oxygen ions from IGZO layer through ZrO_2 layer creating the oxygen vacancy filament play an important role in the forming free resistive switching.

1 Introduction

Recently, resistive random access memory (RRAM) has been widely investigated as next-generation nonvolatile memory devices due to its simple structure, switching speed, low power consumption, long retention time, high density integration and compatibility with complementary metal oxide semiconductor technology [1, 2]. Many oxide materials have been explored as resistive switching (RS) elements which include pure and doped perovskite [3], magnetoelectric oxides [4] and binary transition metal oxides (TMO) [5, 6]. Compared with ternary or quaternary oxide semiconductor films, binary metal oxides have the advantage of a simple fabrication process and are more compatible with complementary metal–oxide semiconductor processing.

The zirconium oxide has obviously excellent characteristics compared with other binary transition metal oxides particularly in retention and on/off ratio. However, the dominant parameter that has to be considered for the application of binary metal oxides is that the nonstoichiometric oxides such as ZrO_x, NiO_x, and Nb_2O_{5-x} show low device yield [7]. Therefore, stoichiometric ZrO_2 is supposed to be a promising candidate for nonvolatile memory device because it has several merits such as simple constituent, high breakdown field, and superior thermal stability [8]. Especially it gives a possible way to solve the problem of low device yield of nonstoichiometric oxides. It is also observed that low temperature growth of ZrO_2 thin film has amorphous nature [9]. Amorphous switching layers may be better RRAM candidates because they offer structural homogeneity and do not require high temperature processing or the epitaxially-matched substrates that are needed for single crystal materials. Indeed, recent reports suggest that amorphous RRAM devices can offer an enhanced reproducibility and better long term stability in comparison to polycrystalline based devices [9, 10].

ZrO_2 with a large optical bandgap (~5.1 eV) are highly transparent in the visible region. Hence, if ZrO_2 can be sandwiched between transparent electrodes and transparent substrates, a fully transparent RRAM (TRRAM) device could be realized and implemented in various electronic systems.

The increasing market for optoelectronic devices has encouraged the use of more available and easily processed materials as alternatives for metallic conductive layers. Metal oxides have been extensively explored in the past few years due to their transparency, which enables scope for extending their applications into transparent electronics. In addition, indium tin oxide (ITO) and F-doped SnO_2 (FTO) films are in the list of transparent electrodes. In and Ga co-doped in ZnO (IGZO) is a new candidate used in optoelectronic devices due to its high transmittance, excellent surface

✉ Bhaumik V. Mistry
bhaumik_phy@yahoo.co.in

[1] Department of Physics, University School of Sciences, Gujarat University, Ahmedabad 380 009, India

smoothness, and low processing temperatures [11]. The utility of IGZO semiconducting thin film as an electrode material for a RRAM device has been shown by Yan et al. [12].

In this study, we report on fabrication of a-IGZO and a-ZrO_2 thin films on quartz substrate by pulse laser deposition technique. The transparent a-ZrO_2/a-IGZO heterojunction for potential application of resistance switching property are discussed.

2 Experimental

The IGZO PLD target was prepared by mixing In_2O_3 (AR, 99.99%), Ga_2O_3 (AR, 99.99%) and ZnO (AR, 99.99%) powders with molar ratio of 1:1:1 and then compressed at room temperature to form a disc. The compressed disc was then sintered for 12 h at 1150 °C. The diameter of the target is 15 mm. Due to very low volatility of In, Ga, and Zn, it can be believed that the target could maintain the same stoichiometry as the mixed powder. Also ZrO_2 target made from zirconium oxide powder ground in pestle mortar and sintering at 1000 °C for 18 h. Quartz was used as substrates, and were ultrasonically cleaned every 10 min by acetone, deionized water and alcohol in turn. Then the substrates were put into a vacuum oven. Firstly IGZO thin films were deposited on ultrasonically cleaned quartz substrate by PLD technique using 3rd harmonic of Nd:YAG laser (λ—355 nm) at oxygen partial pressure of 10 mTorr and 400 °C temperatures. The base pressure of the PLD chamber was 6×10^{-7} Torr. In the deposition process, the pulse repetition rate was kept at 10 Hz and the number of pulses were 20,000. The target–substrate separation was 45 mm. Next, the ZrO_2 thin film was deposited on part of the IGZO thin film by using a shadow mask. Typical substrate temperature and the oxygen partial pressure for this run was kept at 350 °C and 20 mTorr, respectively and number of laser pulses were 25,000.

The a-ZrO_2/a-IGZO heterojunction was characterized by grazing incidence X-ray diffraction (GIXRD, PANalytical X'Pert Pro System), atomic force microscopy (AFM, Nanosurf AG), stylus surface profiler (DekTac. 3.2, Veeco), Hall Effect measurement (Ecopia Corporation, HMS-3000) and current–voltage characteristics using a Source meter (Keithley 2450 SMU). All the measurements were performed at room temperature.

3 Results and discussion

The carrier concentration, resistivity and Hall mobility of bottom transparent electrode IZGO film, determined from the Hall effect measurements, were 8.2×10^{19} cm^{-3}, 4.7×10^{-3} Ω cm and 16.1 cm^2 V^{-1} S^{-1}, respectively. These optimized values of electrical parameters clearly suggest that IGZO is useful as excellent transparent electrode in thin film device application.

Figure 1a, b shows the atomic force microscopy (AFM), images of the IGZO and ZrO_2 thin films. IGZO film shows smooth surface with average surface roughness value of 3.83 nm. Such a smooth surface of the oxide bottom electrode favors the growth of high quality dielectric film, ZrO_2, which is active layer in the present study. The RMS roughness of the ZrO_2/IGZO layer was 9.17 nm. The particle size of the IGZO and ZrO_2 thin film were 80 and 220 nm, respectively, estimated from AFM analysis.

Figure 2 shows the GIXRD of a-IGZO film and ZrO_2/IGZO/Quartz heterojunction. As the deposition temperature of the film is much lower than the crystallization temperatures of either layers viz., ZnO and ZrO_2, we can see that the IGZO film ZrO_2/IGZO/Quartz heterojunction has amorphous state and no other peaks accept a broad hump due quartz substrate is observed. It is reported that the ZrO_2 film crystallizes above 500 °C in to monoclinic and/or tetragonal phase [13]. However, the objective of the present work was to keep the ZrO_2 in complete amorphous phase. Thickness of the ZrO_2 film was 190 nm as measured by using stylus surface profiler.

Figure 3 shows the optical transmission spectra of the a-ZrO_2/a-IGZO heterojunction. The measured average transmittance of the film is greater than 80% in the visible light region. The band gap energy of the a-ZrO_2/a-IGZO heterojunction was derived from the Tauc plot of $(\alpha h\nu)^2$ as a function of the photon energy $h\nu$, as shown in the inset of figure. The band gap of the heterojunction was estimated to be 3.9 eV, which is more than the IGZO (3.1 eV) and less than the ZrO_2 (5.8 eV) films [14]. Yao et al. reported that the a-ZrO_2/a-IGZO heterojunction interface has no valance band offset [14]. Therefore conduction band offset $\Delta E_c = 2.7$ eV is obtained for the a-ZrO_2/a-IGZO heterojunction. Possible energy band diagram of the a-ZrO_2/a-IGZO heterojunction is shown in Fig. 4.

The current–voltage (*I–V*) characteristics of a-ZrO_2/a-IGZO heterojunction were obtained by using stack-capacitor like structure with a system source meter (Keithley SMU 2450). Here Au probes were directly pressed on ZrO_2 and IGZO layer for top and bottom electrodes, respectively, as shown in the inset of the Fig. 5. Figure 5 show typical *I–V* curves of the device at room temperature. The *I–V* curves are non-linear and hysteresis type. The device does not require any forming voltage sweep to activate memory characteristics. First, during the set process, a predetermined sweeping voltage of about 3 V with 10 mA current compliance; was applied and device goes into low resistance state (LRS). In a subsequent sweep, the LRS was achieved during backward sweeping from 3 to 0 V. In a similar fashion during the reset process, the resistance switching (RS) can be restored to

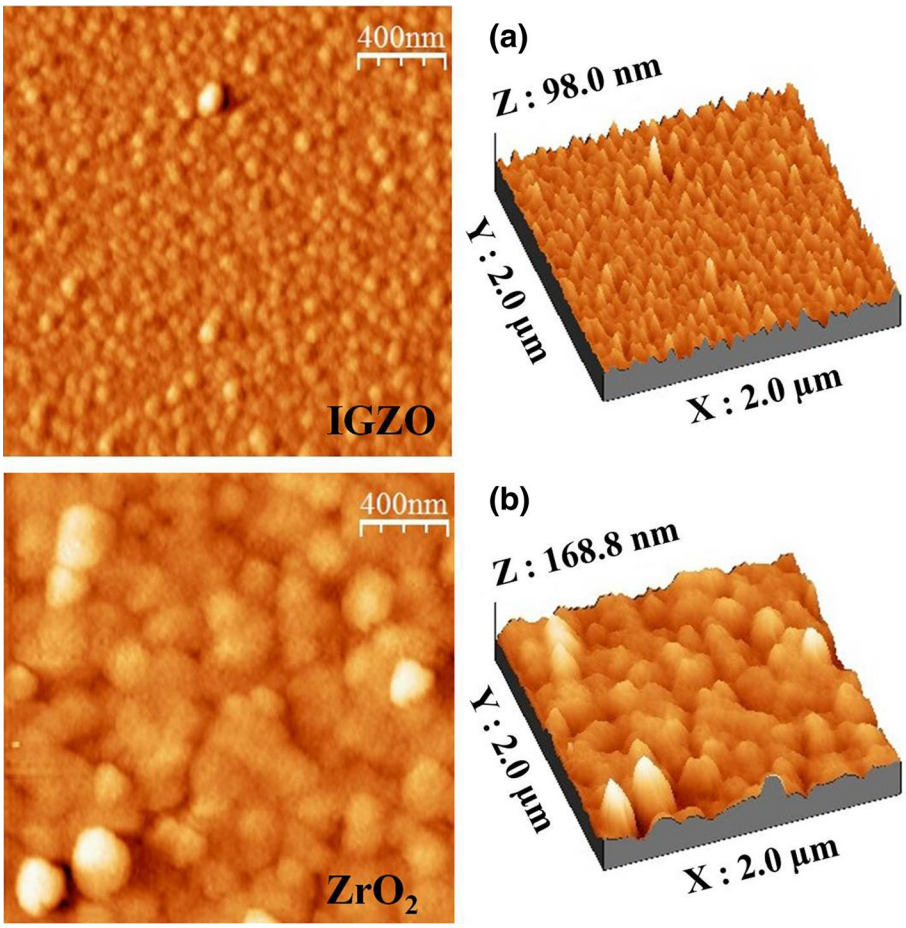

Fig. 1 2-dimensional and 3-dimensional AFM images of **a** IGZO and **b** ZrO_2 thin films

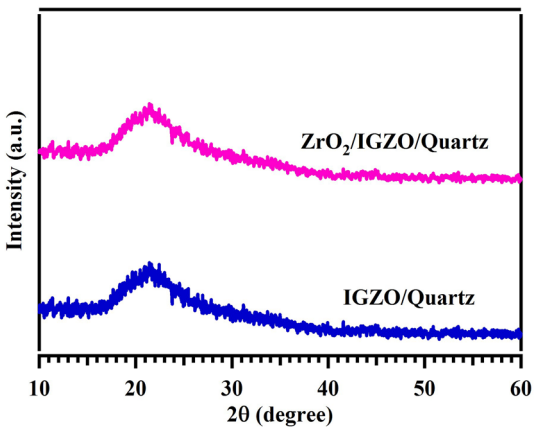

Fig. 2 GIXRD pattern of the IGZO/Quartz and ZrO_2/IGZO/Quartz heterojunction

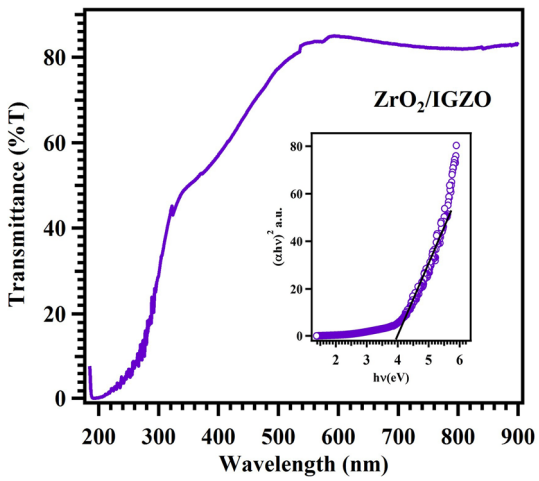

Fig. 3 Optical transmittance spectra and Tauc plot (inset) of ZrO_2/IGZO/Quartz heterojunction

high resistance state (HRS) by using a negative sweeping voltage of about − 3 V. In a subsequent sweep, the HRS was achieved during the backward sweeping from − 3 to 0 V. It is reported that the RS behaviour, i.e., forming as well as unipolar and bipolar type RS in ZrO_2 films strongly depend upon the electrodes, for example, Au/ZrO_2/Ag, metal/NiO/metal as well as TiN/ZrO_2/Pt RRAM devices show forming free, bipolar RS [15–17], similar to the present study; while Al/ZrO_2/Al and Pt/ZrO_2/*p*-Si devices reported to exhibit the unipolar RS with requirement of forming process [18,

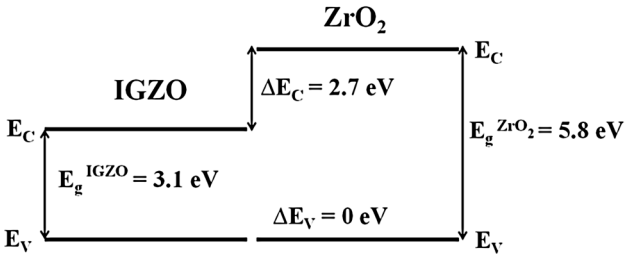

Fig. 4 Schematic of energy band diagram of a-ZrO_2/a-IGZO heterojunction

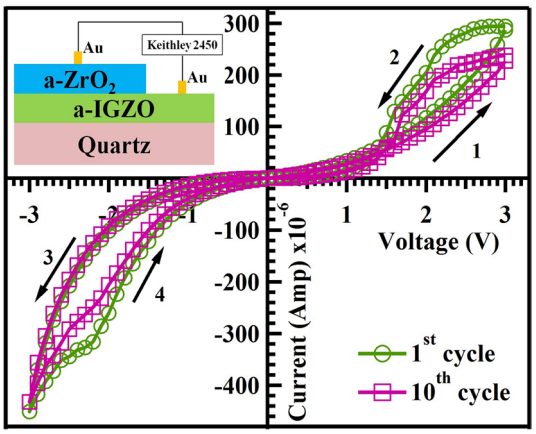

Fig. 5 Typical *I–V* characteristics of the a-ZrO_2/a-IGZO heterojunction for resistive switching properties

19]. However, in each of the previous reports metal pairs were used top and bottom electrodes giving non-transparent RRAM device; where as in our case the bottom electrode IGZO is highly transparent and therefore suitable for transparent RRAM. The cycling endurance characteristics of the ZrO_2/IGZO structure measured in dc sweep mode up to 50th RS cycles which shows that the memory device can be switched continuously between the LRS and the HRS without exhibiting any operation failure.

For the RS mechanism, studies have indicated that the bipolar resistance switching is related to the redox reaction near the anode–electrode/oxide interface [1]. Moreover, the creation of oxygen vacancies in the ZrO_2 lattice at the Au/ZrO_2 interface is responsible for the RS. Bipolar resistive switching generally depends on the formation and rupture of conductive filaments in the oxide layer. Conducting bottom oxide layer may be suggested as the oxygen supplier [3, 6]. Based on the resistance switching behaviour, a model is proposed to explain the resistance switching mechanism and is schematically shown in Fig. 6. The formation of conductive filaments through oxygen vacancies during the positive bias of set step can be understood in terms of migration of O_2 ions from the bottom electrode IGZO towards the top electrode Au. This migration of O_2 ions is capable of generating O_2 vacancies in the bulk of ZrO_2 and interfacial layer which can arrange themselves and connect under the applied bias to form conducting filaments and hence provide easy path for the flow of electrons. During the negative bias O_2 ions

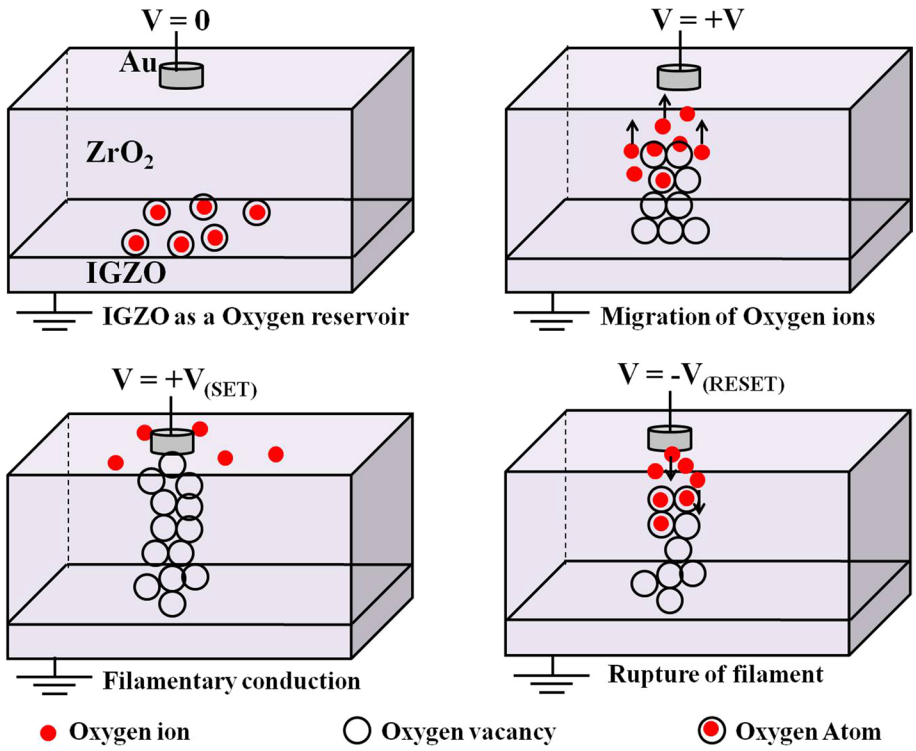

Fig. 6 Physical model of resistive switching mechanism of the Au/ZrO_2/IGZO structure

repelled back to bottom electrode and thus cause the annihilation of oxygen vacancies or oxidation of the conductive paths. This can rupture the conductive filament and device restored to the HRS. When positive bias is applied again to the top electrode, oxygen ions are once again attracted towards it creating oxygen vacancies behind which involve themselves to complete the ruptured filaments under the applied bias during SET step and provide easy path for the flow of electron leading to low resistance ON-state. The oxygen ions migrate between the interfacial layer and ZrO_2 film dominating the state to LRS or HRS under applied bias. The switching mechanism of the Au/ZrO_2/IGZO is similar to the ITO/Eu_2O_3/FTO, Pt/GO/ITO and Au/TiO_2/FTO devices that the formation and rupture of conductive filaments in the oxide layer [20–22]. The oxygen ions are not able to migrate absolutely homogeneously. The inhomogeneous conducting path of oxygen ion vacancy might be polarity dependent which attribute to the asymmetric behaviour in the I–V curves as the voltage was swept from 0 to + 3 V and to − 3 V. Further the conducting paths/filaments and its diameters may vary with probe contact area as that vary the electric field beneath the contact which in turn lead to varying resistance switching. Such an investigation need to be carry out for replacing the top metal electrode by transparent conducting electrode in order to obtain fully transparent RRAM device. Thus IGZO electrodes are expected to play vital role in the resistive switching process of ZrO_2. Similar role of oxide bottom electrode in the RS of ITO/V_2O_5/ITO has been reported recently [23].

4 Summary and conclusions

In summary, a-ZrO_2/a-IGZO heterojunction has been successfully fabricated on quartz substrate using pulse laser deposition. Smooth surface morphology and amorphous nature of the structure was confirmed with AFM and GIXRD. The transparent a-ZrO_2/a-IGZO device showed more than 80% transparency in the visible range. Forming free bipolar RS was confirmed and the SET and RESET transitions were observed for positive and negative voltages, respectively, such that RS occurs as positive oxygen vacancies migrate towards (SET) and away (RESET) from the Au/ZrO_2 interface. Formation and rupture of the conducting filaments due to oxygen vacancy is attributed to the observed resistance switching phenomenon. Our results show that a-ZrO_2/a-IGZO heterojunction has a potential for future candidate of TRRAM.

References

1. A. Sawa, Mater. Today **11**, 28–36 (2008)
2. L. Wang, C.H. Yang, J. Wen, S. Gai, Y.X. Peng, J. Mater. Sci. Mater. Electron. **26**, 4618 (2015)
3. N.C. Pandya, A.K. Debnath, U.S. Joshi, J. Phys. D **49**, 055301 (2016)
4. T. Nakamura, K. Homma, K. Tachibana, Nanoscale Res. Lett. **8**, 76 (2013)
5. U.S. Joshi, S.J. Trivedi, K.H. Bhavsar, U.N. Trivedi, S.A. Khan, D.K. Avasthi, J. Appl. Phys. **105**, 073704 (2009)
6. B.V. Mistry, R. Pinto, U.S. Joshi, J. Mater. Sci. Mater. Electron. **27**, 1812 (2016)
7. D.S. Lee, D.J. Seong, H.J. Choi, I. Jo, R. Dong, W. Xiang, S.K. Oh, M.B. Pyun, S.O. Seo, S.H. Heo, M.S. Jo, D.K. Hwang, H.K. Park, M. Chang, M. Hasan, H.S. Hwang, in *Technical Digest—International Electron Devices Meeting*, 2006, p. 439
8. P. Zhou, H. Shen, J. Li, L.Y. Chen, C. Gao, Y. Lin, T.A. Tang, Thin Solid Films **518**, 5652 (2010)
9. P. Parreira, G.W. Paterson, S. McVitie, D.A. MacLaren, J. Phys. D **49**, 095111 (2016)
10. Y. Kang, T. Lee, K. Moon, J. Moon, K. Hong, J. Cho, W. Lee, J. Myoung, Mater. Chem. Phys. **138**, 623 (2013)
11. B.V. Mistry, J. Mistry, U.N. Trivedi, V.G. Joshi, U.S. Joshi, AIP Conf. Proc. **1512**, 988 (2013)
12. X.B. Yan, H. Hao, Y.F. Chen, Y.C. Li, W. Banerjee, Appl. Phys. Lett. **105**, 093502 (2014)
13. Y. Gao, Y. Masuda, H. Ohta, K. Koumoto, Chem. Mater. **16**, 2615–2622 (2004)
14. J. Yao, S. Zhang, L. Gong, Appl. Phys. Lett. **101**, 093508 (2012)
15. Y. Li, S. Long, M. Zhang, Q. Liu, L. Shao, S. Zhang, Y. Wang, Q. Zuo, S. Liu, M. Liu, IEEE Electron Device Lett. **31**(2), 117–119 (2010)
16. T. Ishihara, I. Ohkubo, K. Tsubouchi, H. Kumigashira, U.S. Joshi, Y. Matsumoto, H. Koinuma, M. Oshima, Mater. Sci. Eng. B **148**(1–3), 40–42 (2008)
17. B. Sun, Y.X. Liu, L.F. Liu, N. Xu, Y. Wang, X.Y. Liu, R.Q. Han, J.F. Kang, J. Appl. Phys. **105**, 061630 (2009)
18. X. Wu, P. Zhou, J. Li, L.Y. Chen, H.B. Lv, Y.Y. Lin, T.A. Tang, Appl. Phys. Lett. **90**(18), 183507 (2007)
19. D. Lee, H. Choi, H. Sim, D. Choi, H. Hwang, M.J. Lee, S.A. Seo, I.K. Yoo, IEEE Electron Device Lett. **26**(10), 719–721 (2005)
20. T. Zhang, X. Ou, W. Zhang, J. Yin, Y. Xia, Z. Liu, J. Phys. D **47**, 065302 (2014)
21. G. Khurana, P. Mishra, R.S. Katiyar, J. Appl. Phys. **114**, 124508 (2013)
22. D. Chu, A. Younis, S. Li, J. Phys. D **45**, 355306 (2012)
23. Z. Wan, R.B. Darling, A. Majumdar, M.P. Anantram, Appl. Phys. Lett. **111**, 041601 (2017)